EUROPEAN JOURNAL OF PURE AND APPLIED MATHEMATICS
2026, Vol. 19, Issue 2, Article Number 6717
ISSN 1307-5543 – ejpam.com
Published by New York Business Global

A Novel Study for the Spread of COVID-19 via Fractional Derivative: A New Perspective of Hybrid Stochastic Approach

Riaz Ahmad[1,*], Junyi Zhu[1], Zhoujun Ju[1], Kuizhuang Chen[1], Xinyu Mei[1], Asma Farooqi[1], Ghulam Bary[2], Wei Sin Koh[3], Ilyas Khan[4]

[1] *School of Mathematics and Statistics, Nanjing University of Information Science and Technology, 210044; and Reading Academy, Nanjing University of Information Science and Technology, Nanjing, P. R. China*
[2] *Faculty of Science, Yibin University, Yibin 644000, Sichuan, China*
[3] *INTI International University, Persiaran Perdana BBN Putra Nilai, 71800 Nilai, Negeri Sembilan, Malaysia*
[4] *Department of Mathematics, College of Science, Al-Zulfi, Majmaah University, Al-Majmaah, Majmaah 11952, Saudi Arabia*

Abstract. In the present research, we address and improve a hybrid technique that combines the Caputo and Atangana-Baleanu formulations for a stochastic fractional differential equation applied to a chaotic framework. We primarily demonstrate the existence and uniqueness of solutions before presenting a new numerical scheme for the Caputo and Atangana-Baleanu derivatives. Our quantitative and qualitative study is centered on a stochastic model of COVID-19 transmission and prevention, which classifies the population of an involved region into susceptible, exposed, infected (symptomatic and asymptomatic), treated, and recovered groups. Considering the natural unpredictability of illness progression, the number of symptomatic patients, fatalities, and recoveries is represented as stochastic processes. Therefore, the governing equations have to incorporate stochasticity. We construct stochastic differential and integral equations from the fundamental nonlinear systems and analytically analyze their existence and uniqueness. For various fractional orders, numerical simulations are conducted, and the outcomes for the Caputo and Atangana-Baleanu situations are thoroughly examined. We also provide numerical calculations with projected and reasonable parameters for different fractional orders of the Caputo derivative. The understanding of disease behavior under presented hybrid frameworks is improved by the fractional-order analysis, which is reinforced by simulation data and offers insightful information about the dynamics of COVID-19.

2020 Mathematics Subject Classifications: 34A08, 37H10, 92D30

Key Words and Phrases: fractional differential equations, stochastic models, COVID-19 transmission, Caputo derivative, Atangana-Baleanu derivative

*Corresponding Author.
DOI: https://doi.org/10.29020/nybg.ejpam.v19i2.6717

Email addresses: riazgill2007@gmail.com (R. Ahmad)

1. Introduction

The interdisciplinary approach entails a variety of epidemic and mathematical models that are useful to explore wide infections with data from biomathematical sciences. The popularity of this topic demonstrates its significance. Numerous mathematical models were established, which include SI, SIR, SIS, SARS, SIER, H1N1, HBV, H5N1, and so on [1, 2]. These mathematical models give rational predictions and knowledge about the disease that is more helpful for society's well-being [3–8]. The indispensable and significant problems are the stability and mitigation of numerous infections in human communities. As an outcome, every epidemiological infection is transformed into a mathematical model as swiftly as possible, and the study of this modeling was entrenched to devise and implement. Initially, McKendrick and Kermack [9, 10] studied the pre-epidemic models and examined the details for disease surveillance. Several scholars have been using this basic and essential approach to examine the epidemic models as SEIS, SEIRS, SIRS, vaccine-related, and other stay models by incorporating various vaccination and delay-time factors [11–13].

A prominent invention in focusing on various infectious diseases is the mathematical modeling approach [14–17]. Stochastic differential equations could be used to deal with a variety of issues and challenges in the sciences and technology [18–20]. In physics, chemistry, fluid dynamics, and epidemiological modeling, fractional differential equations are extensively employed [21, 22]. The most challenging aspect of understanding viral infections is forecasting disease characteristics and the number of individuals who are affected in the future. Many researchers from a wide range of interdisciplinary domains, including statistics and engineering disciplines, have been studying on observing this kind of assumption, making it a fascinating subject of the research article. Many investigations are mainly concentrating on identifying the mechanisms of COVID-19 as it evolved into an infectious disease. To compute the cumulative number of infections and fatalities, dynamic models are employed to represent epidemic waves and the time of action. COVID-19 transmission rates vary by nation in all research studies, as do virus dynamics, which have been affected by individual behaviors, temperature, relative air humidity, and wind speed. Authorities have made more efficient and effective efforts to reduce human and economic losses based on these projections and research findings.

The continuation of classical calculus is fractional calculus. Non-integer order operators in mathematical models help readers understand and interpret a phenomenon. Models with fractional-order derivatives can also depict etiolate conditions and crossover etiquette with considerable accuracy. Mathematical models incorporating fractional derivatives yield additional information about a disease [23–26]. In the research [27, 28], various fractional operators, as well as singular and non-singular kernels, were presented. These fractional operators' applications and references can be found in contemporary literature [29–31]. Recently, there has not been much work done on COVID-19 mathematical models; however, certain developments on fractional-order operators have been recommended. Khan and Atangana [32] ascertain the dynamics of (2019-nCoV) fractional derivatives to understand the epidemic status in Wuhan. The researchers look at the results of a fractional derivative bio-mathematical modeling for hepatitis C [33]. The COVID-19 approach is described, along with its dynamical investigation by applying the fuzzy Caputo differential equation [34]. The TB dynamics in relapse were contemplated, as the writer adopted conformable derivatives to assess the data [35]. Many researchers aim to explore some intriguing results relating to fractional derivative calculus and its relationship to numerous physical structures [36]. The study explained the numerically stable findings for a fractional derivative HIV/AIDS model [37]. Morales et.al. discuss the subject of oxygen diffusion in many fractional operators [38]. It investigated the application of a new fractional-fractal operator with distinctive and nonsingular kernels to generate a dynamical coronavirus model [39]. Baleanu et al. closely studied the dynamical research of coronary models in fractional derivatives employing an exponential kernel [40]. Recently, Tuan et. al. investigated a fractional-order COVID-19 model in the Caputo way [41]. Saleem et. al. seek to explore the latest analysis on coronavirus-infected cases in Saudi Arabia [42]. The work on epidemiological analysis opens the door for mathematical modeling of other pandemic diseases [43–48].

We outline a specific hybrid stochastic mathematical COVID-19 framework to analyze the outcome of environmental factors on COVID-19 spread and improve the current research to real-world problems. After that, the categorical imperatives for population decline and durability. are investigated. Moreover, the current stochastic COVID-19 model's threshold is proposed. When there is small or huge noise, it serves a crucial role as a backbone in mathematical models. Finally, we use MATLAB to see the numerical simulations graphically.

2. Mathematical System with Differential and Integral Operators

Mathematical interpretation of differential as well as integral operators having singular and non-singular kernels are defined as [3]

$$ {}_0^C D_t^\alpha g(t) = \frac{1}{\Gamma(1-\alpha)} \int_0^t \frac{d}{d\varsigma} g(\varsigma)(t-\varsigma)^{-\alpha} d\varsigma, \quad 0<\alpha<1, \tag{1} $$

$$ {}_0^{CF} D_t^\alpha g(t) = \frac{M(\alpha)}{1-\alpha} \int_0^t \frac{d}{d\varsigma} g(\varsigma) e^{-\frac{\alpha}{1-\alpha}(t-\varsigma)} d\varsigma, \tag{2} $$

$$ {}_0^{ABC} D_t^\alpha g(t) = \frac{AB(\alpha)}{1-\alpha} \int_0^t \frac{d}{d\varsigma} g(\varsigma) E_\alpha \left[-\frac{\alpha}{1-\alpha}(t-\varsigma)^\alpha \right] d\varsigma. \tag{3} $$

Further, the fractional integral operators are defined with Mittag-Leffer, power law, and exponential decay

$$ {}_0^C I_t^\alpha g(t) = \frac{1}{\Gamma(\alpha)} \int_0^t (t-\varsigma)^{\alpha-1} g(\varsigma) d\varsigma, \tag{4} $$

$$ {}_0^{CF} I_t^\alpha g(t) = \frac{1-\alpha}{M(\alpha)} g(t) + \frac{\alpha}{M(\alpha)} \int_0^t g(\varsigma) d\varsigma, \tag{5} $$

$$ {}_{0}^{AB}I_t^{\alpha} g(t) = \frac{(1-\alpha)}{AB(\alpha)} g(t) + \frac{\alpha}{AB(\alpha)\Gamma(\alpha)} \int_0^t (t-\varsigma)^{\alpha-1} g(\varsigma) d\varsigma. \tag{6} $$

The purpose of defined integrals is to enhance the degree of freedom in polynomials to fit our model for a given data to achieve accurate results.

3. Mathematical Setup-Covid-19

We take into account the transmission of COVID-19 by dividing the population into five principal groups, as shown in Table 1, along with definitions of variables/parameters. The Infectious class is defined as considering the transmission rate function

$$ \lambda = \beta \left(I(t) + \phi_1 T(t) + \phi_2 A(t) \right), \tag{7} $$

where ϕ_1 and ϕ_2 are indeed the infectiousness mitigation parameters. People in the class T are in a restricted condition, hence they are less contagious than those in group A: Therefore

$$ 0 \leq \phi_1 \leq \phi_2 \leq 1. \tag{8} $$

The flow chart can be seen in Fig. 1:

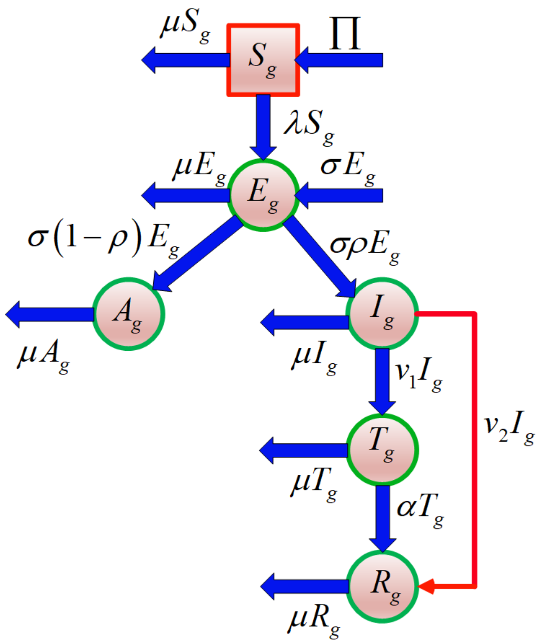

Figure 1: Flowchart of $S_gE_gA_gI_gT_gR_g$ model for COVID-19.

Considering the specifications in Table 1, with Fig. 1, and conditions, the non-linear ordinary differential equations are as described in the following:

Table 1: Summary of the variables with description.

Variables	Narration
$S_g(t)$	Susceptible group
$E_g(t)$	Exposed group
$I_g(t)$	Symptomatic and infected group
$A_g(t)$	Infected but asymptomatic group
$T_g(t)$	Treated group
$R_g(t)$	Recovered group

$$\left.\begin{aligned} S_g' &= \pi - \lambda S_g - \mu S_g \\ E_g' &= \lambda S_g - Q_1 E_g \\ I_g' &= \sigma\rho E_g - Q_2 I_g \\ A_g' &= \sigma(1-\rho)E_g - \mu A_g \\ T_g' &= \nu_1 I_g - Q_3 T_g \\ R_g' &= \nu_2 I_g + \alpha T_g - \mu R_g \end{aligned}\right\} \tag{9}$$

where $Q_1 = (\mu + \sigma)$, $Q_2 = (\mu + \nu_1 + \nu_2)$, $Q_3 = \alpha + \mu$ and the conditions are

$$\{S_g(0) > 0, E_g(0), I_g(0), A_g(0), T_g(0), R_g(0)\} \geq 0. \tag{10}$$

The mass balance constraint is satisfied:

$$\frac{d}{dt}(S_g + E_g + I_g + A_g + T_g + R_g) = \pi - \mu(S_g + E_g + I_g + A_g + T_g + R_g) \tag{11}$$

The recovered group is considered extra. We consider all the parameters used in our model to be positive over time.

4. The Hybrid Stochastic Model Technique Using ABC

We introduce the hybrid influence of environmental white noise [3] to change the suggested deterministic COVID-19 model Eq. 9 into a stochastic model. It is accomplished by incorporating non-linear perturbations into the full system equations. We just changed the rate of each group, as defined

$$\begin{aligned} S_g(t): &\quad -\lambda \longrightarrow -\lambda + (\Lambda_{11}S_g + \Lambda_{12})\,\beta_1(t) \\ E_g(t): &\quad -\sigma \longrightarrow -\sigma + (\Lambda_{21}E_g + \Lambda_{22})\,\beta_2(t) \\ I_g(t): &\quad -\nu_1 \longrightarrow -\nu_1 + (\Lambda_{31}I_g + \Lambda_{32})\,\beta_3(t) \\ A_g(t): &\quad -\mu \longrightarrow -\mu + (\Lambda_{41}A_g + \Lambda_{42})\,\beta_4(t) \\ T_g(t): &\quad -\alpha \longrightarrow -\alpha + (\Lambda_{51}T_g + \Lambda_{52})\,\beta_5(t). \end{aligned} \tag{12}$$

where $\beta_i(t)$ is Brownian motion and Λ_{ij} for $i, j = 1, 2, ..5$ is positive and sourronding perturbation. Hence, the stochastic model is written as

$$\left.\begin{array}{rl} dS_g & = [\pi - (\lambda + \mu)S_g]dt + (\Lambda_{11}S_g + \Lambda_{12})\,S_g d\beta_1(t) \\ dE_g & = [\lambda S_g - Q_1 E_g]\,dt + (\Lambda_{21}E_g + \Lambda_{22})\,E_g d\beta_2(t) \\ dI_g & = [\sigma\rho E_g - Q_2 I_g]\,dt + (\Lambda_{31}I_g + \Lambda_{32})\,I_g d\beta_3(t) \\ dA_g & = [\sigma(1-\rho)E_g - \mu A_g]dt + (\Lambda_{41}A_g + \Lambda_{42})\,A_g d\beta_4(t) \\ dT_g & = [\nu_1 I_g - Q_3 T_g]\,dt + (\Lambda_{51}T_g + \Lambda_{52})\,T_g d\beta_5(t). \end{array}\right\} \tag{13}$$

4.1. Existence and Uniqueness of Solutions for the Stochastic Model

We establish the existence and uniqueness of solutions for the stochastic differential equation system (13) through rigorous mathematical analysis, addressing the local Lipschitz and linear growth conditions required by standard SDE theory.

Next to prove that the stochastic differential equation system (13) admits a unique strong solution on bounded domains.

Proof We verify the conditions of the standard existence-uniqueness theorem for SDEs by establishing local Lipschitz continuity and linear growth conditions for both drift and diffusion coefficients.

Step 1: Define a Domain

For any given $R > 0$, we define the bounded domain:

$$D_R = \{X = (S_g, E_g, I_g, A_g, T_g) \in \mathbb{R}^5_+ : |X| \leq R, \sum_i X_i \leq N\} \tag{14}$$

where N represents a reasonable upper bound for the total population.

On D_R, the transmission rate function has a definite bound:

$$|\lambda| = |\beta(I_g + \phi_1 T_g + \phi_2 A_g)| \leq \beta(1 + \phi_1 + \phi_2)R =: C_R \tag{15}$$

Step 2: Local Lipschitz Conditions for Drift Terms

For the drift function $G_1(X, t) = \pi - (\lambda + \mu)S_g$, let $X, Y \in D_R$ with corresponding transmission rates λ and $\lambda^{(1)}$. Then:

$$\begin{aligned} |G_1(X,t) - G_1(Y,t)|^2 &= |-(\lambda+\mu)S_g + (\lambda^{(1)} + \mu)S_g^{(1)}|^2 \\ &= |-(\lambda+\mu)(S_g - S_g^{(1)}) - (\lambda - \lambda^{(1)})S_g^{(1)}|^2 \\ &\leq 2|(\lambda+\mu)|^2|S_g - S_g^{(1)}|^2 + 2|\lambda - \lambda^{(1)}|^2|S_g^{(1)}|^2 \end{aligned} \tag{16}$$

Since $|\lambda - \lambda^{(1)}| = \beta|(I_g - I_g^{(1)}) + \phi_1(T_g - T_g^{(1)}) + \phi_2(A_g - A_g^{(1)})| \leq \beta(1+\phi_1+\phi_2)|X - Y|$, we obtain:

$$|G_1(X,t) - G_1(Y,t)|^2 \leq L_1|X - Y|^2 \tag{17}$$

where $L_1 = 2(C_R + \mu)^2 + 2\beta^2(1 + \phi_1 + \phi_2)^2 R^2$.

Similarly, for the remaining drift terms:

$$L_2 = 2(\beta(1 + \phi_1 + \phi_2)R + Q_1)^2 + 2\beta^2(1 + \phi_1 + \phi_2)^2 R^2 \tag{18}$$

$$L_3 = 2(\sigma\rho R + Q_2)^2 \tag{19}$$

$$L_4 = 2(\sigma(1-\rho)R + \mu)^2 \tag{20}$$

$$L_5 = 2(\nu_1 R + Q_3)^2 \tag{21}$$

Step 3: Local Lipschitz Conditions for Diffusion Terms

For the diffusion function $H_1(X,t) = (\Lambda_{11}S_g + \Lambda_{12})S_g$, we use algebraic factorization:

$$|H_1(X,t) - H_1(Y,t)| = |(\Lambda_{11}S_g + \Lambda_{12})S_g - (\Lambda_{11}S_g^{(1)} + \Lambda_{12})S_g^{(1)}| \tag{22}$$

Expanding the difference:

$$\begin{aligned} H_1(X,t) - H_1(Y,t) &= \Lambda_{11}S_g^2 + \Lambda_{12}S_g - \Lambda_{11}(S_g^{(1)})^2 - \Lambda_{12}S_g^{(1)} \\ &= \Lambda_{11}(S_g^2 - (S_g^{(1)})^2) + \Lambda_{12}(S_g - S_g^{(1)}) \\ &= \Lambda_{11}(S_g - S_g^{(1)})(S_g + S_g^{(1)}) + \Lambda_{12}(S_g - S_g^{(1)}) \\ &= (S_g - S_g^{(1)})[\Lambda_{11}(S_g + S_g^{(1)}) + \Lambda_{12}] \end{aligned} \tag{23}$$

Taking the modulus and applying bounds on D_R where $|S_g|, |S_g^{(1)}| \leq R$:

$$\begin{aligned} |H_1(X,t) - H_1(Y,t)| &= |S_g - S_g^{(1)}| \cdot |\Lambda_{11}(S_g + S_g^{(1)}) + \Lambda_{12}| \\ &\leq |S_g - S_g^{(1)}| \cdot [|\Lambda_{11}|(|S_g| + |S_g^{(1)}|) + |\Lambda_{12}|] \\ &\leq |S_g - S_g^{(1)}| \cdot [|\Lambda_{11}|(R + R) + |\Lambda_{12}|] \\ &= (2|\Lambda_{11}|R + |\Lambda_{12}|)|S_g - S_g^{(1)}| \\ &\leq \tilde{L}_1|X - Y| \end{aligned} \tag{24}$$

where $\tilde{L}_1 = 2|\Lambda_{11}|R + |\Lambda_{12}|$.

For the remaining diffusion terms:

$$\tilde{L}_\ell = 2|\Lambda_{\ell 1}|R + |\Lambda_{\ell 2}|, \quad \ell = 2,3,4,5 \tag{25}$$

Step 4: Local Linear Growth Conditions

Drift terms: For G_1 on D_R:

$$|G_1(X,t)|^2 = |\pi - (\lambda + \mu)S_g|^2 \leq 2\pi^2 + 2(C_R + \mu)^2R^2 \leq K_1(1 + |X|^2) \tag{26}$$

where $K_1 = 2\pi^2 + 2(C_R + \mu)^2R^2$.

Diffusion terms: For H_1, since $|S_g| \leq R$ on D_R:

$$\begin{aligned} |H_1(X,t)|^2 &= |(\Lambda_{11}S_g + \Lambda_{12})S_g|^2 \leq 2\Lambda_{11}^2|S_g|^4 + 2\Lambda_{12}^2|S_g|^2 \\ &\leq 2\Lambda_{11}^2R^4 + 2\Lambda_{12}^2R^2 \leq \tilde{K}_1(1 + |X|^2) \end{aligned} \tag{27}$$

where $\tilde{K}_1 = 2\Lambda_{11}^2R^4 + 2\Lambda_{12}^2R^2$ is constant on D_R.

Similar bounds hold for G_ℓ and H_ℓ, $\ell = 2,3,4,5$.

Step 5: Application of Standard SDE Theory

Since on the bounded domain D_R:

(i) All drift coefficients G_ℓ satisfy local Lipschitz conditions with constants L_ℓ

(ii) All diffusion coefficients H_ℓ satisfy local Lipschitz conditions with constants $\tilde{L}_\ell$

(iii) Linear growth conditions are satisfied locally with constants K_ℓ and $\tilde{K}_\ell$

By the standard existence-uniqueness theorem for SDEs, there exists a stopping time $\tau_R > 0$ such that system (13) has a unique strong solution on $[0, \tau_R]$.

Hence, system (13) admits a unique local strong solution on the bounded domain D_R. Under reasonable parameter assumptions, global existence can be established through appropriate Lyapunov analysis.

5. Numerical Solution-Atangana-Seda Modified Scheme

The improved version of the Atangana-Seda numerical model is discussed in the following section. These Newton polynomial-based techniques will then be utilized to produce numerical interpretation for the model 9 with alternative operators. We address the parameter indexing inconsistency and time-state matching issues identified in the original implementation.

5.1. Corrected Parameter Indexing

We first correct the parameter inconsistency in the stochastic differential equation system. The corrected form of equation (13) ensures consistent indexing throughout:

$$dS_g = [\pi - (\lambda + \mu)S_g]dt + (\Lambda_{11}S_g + \Lambda_{12})S_g d\beta_1(t) \tag{28}$$
$$dE_g = [\lambda S_g - Q_1 E_g]dt + (\Lambda_{21}E_g + \Lambda_{22})E_g d\beta_2(t) \tag{29}$$
$$dI_g = [\sigma\rho E_g - Q_2 I_g]dt + (\Lambda_{31}I_g + \Lambda_{32})I_g d\beta_3(t) \tag{30}$$
$$dA_g = [\sigma(1-\rho)E_g - \mu A_g]dt + (\Lambda_{41}A_g + \Lambda_{42})A_g d\beta_4(t) \tag{31}$$
$$dT_g = [\nu_1 I_g - Q_3 T_g]dt + (\Lambda_{51}T_g + \Lambda_{52})T_g d\beta_5(t) \tag{32}$$

5.2. Modified Adams-Bashforth Implementation

By considering the standard differential equation form:

$$\frac{df(t)}{dt} = y(t, f(t)) \tag{33}$$

The corrected three-step Adams-Bashforth scheme addresses the time-state matching issue:

$$f^{m+1} = f^m + \frac{\Delta t}{12}[23y(t_m, f^m) - 16y(t_{m-1}, f^{m-1}) + 5y(t_{m-2}, f^{m-2})] \tag{34}$$

where the previous values are obtained through: Initial values are computed using Runge-Kutta 2nd order

$$k_1^{(0)} = y(t_0, f^0), \quad k_2^{(0)} = y(t_0 + \Delta t, f^0 + \Delta t k_1^{(0)}) \tag{35}$$

$$f^1 = f^0 + \frac{\Delta t}{2}(k_1^{(0)} + k_2^{(0)}) \tag{36}$$

$$k_1^{(1)} = y(t_1, f^1), \quad k_2^{(1)} = y(t_1 + \Delta t, f^1 + \Delta t k_1^{(1)}) \tag{37}$$

$$f^2 = f^1 + \frac{\Delta t}{2}(k_1^{(1)} + k_2^{(1)}) \tag{38}$$

This ensures consistency between time arguments and state variables throughout the computation.

5.3. Atangana-Seda Using Caputo-Fabrizio Derivative

The Caputo-Fabrizio (CF) derivative is given as

$${}_0^{CF}D_t^{\alpha} f(t) = y(t, f(t)) \tag{39}$$

According to the CF integral, Eq. (39) is written as

$$f(t) - f(0) = \frac{1-\alpha}{M(\alpha)} y(t, f(t)) + \frac{\alpha}{M(\alpha)} \int_0^t y(\tau, f(\tau)) d\tau \tag{40}$$

At $t_{m+1} = (m+1)\Delta t$, the system is redefined as

$$f(t_{m+1}) - f(0) = \frac{1-\alpha}{M(\alpha)} y(t_{m+1}, f(t_{m+1})) + \frac{\alpha}{M(\alpha)} \int_0^{t_{m+1}} y(\tau, f(\tau)) d\tau \tag{41}$$

At $t_m = m\Delta t$

$$f(t_m) - f(0) = \frac{1-\alpha}{M(\alpha)} y(t_m, f(t_m)) + \frac{\alpha}{M(\alpha)} \int_0^{t_m} y(\tau, f(\tau)) d\tau \tag{42}$$

By subtracting the equations and applying the corrected Adams-Bashforth approximation to the integral term:

$$\int_{t_m}^{t_{m+1}} y(\tau, f(\tau)) d\tau \approx \frac{\Delta t}{12}[23y(t_m, f^m) - 16y(t_{m-1}, f^{m-1}) + 5y(t_{m-2}, f^{m-2})] \tag{43}$$

We obtain the modified CF scheme:

$$\begin{aligned} f(t_{m+1}) - f(t_m) = {} & \frac{1-\alpha}{M(\alpha)}[y(t_{m+1}, f(t_{m+1})) - y(t_m, f(t_m))] \\ & + \frac{\alpha \Delta t}{12M(\alpha)}[23y(t_m, f^m) - 16y(t_{m-1}, f^{m-1}) + 5y(t_{m-2}, f^{m-2})] \end{aligned} \tag{44}$$

5.4. Modified Model for Atangana-Seda Via Atangana Baleanu Operator

We have taken into consideration the derivative

$$\begin{cases} {}_0^{ABC}D_t^{\alpha} f(t) = y(t, f(t)) \\ f(0) = f_0 \end{cases} \tag{45}$$

With the help of the Atangana Baleanu (ABC) integral, this equation can be expressed as

$$f(t) - f(0) = \frac{1-\alpha}{AB(\alpha)} y(t, f(t)) + \frac{\alpha}{AB(\alpha)\Gamma(\alpha)} \int_0^t y(\tau, f(\tau))(t-\tau)^{\alpha-1} d\tau \tag{46}$$

Following the Newton polynomial approach and ensuring time-state consistency, the discrete form becomes:

$$\begin{aligned} f(t_{m+1}) = f(0) + \frac{1-\alpha}{AB(\alpha)} y(t_{m+1}, f^{m+1}) \\ + \frac{\alpha(\Delta t)^{\alpha}}{AB(\alpha)\Gamma(\alpha+1)} \sum_{l=0}^{m} w_{l,m+1} y(t_l, f^l) \end{aligned} \tag{47}$$

where the weights $w_{l,m+1}$ are computed using the corrected polynomial interpolation scheme:

$$w_{0,m+1} = (m+1)^{\alpha} - m^{\alpha} \tag{48}$$

$$w_{l,m+1} = (m+1-l)^{\alpha} - 2(m-l)^{\alpha} + (m-1-l)^{\alpha}, \quad 1 \le l \le m \tag{49}$$

$$w_{m+1,m+1} = 1 \tag{50}$$

The weights satisfy the property:

$$\sum_{l=0}^{m+1} w_{l,m+1} = \frac{(m+1)^{\alpha}}{\alpha} \tag{51}$$

5.5. Application: Numerical Approach to the COVID-19 Model

The corrected numerical approach is applied to solve our system. By applying the CF fractional derivative with parameter consistency:

$${}_0^{CF}D_t^{\alpha} S_t = \pi - [\beta(I_t + \phi_1 T_t + \phi_2 A_t) + \mu] S_t \tag{52}$$

$${}_0^{CF}D_t^{\alpha} E_t = \beta(I_t + \phi_1 T_t + \phi_2 A_t) S_t - Q_1 E_t \tag{53}$$

$${}_0^{CF}D_t^{\alpha} I_t = \sigma\rho E_t - Q_2 I_t \tag{54}$$

$${}_0^{CF}D_t^{\alpha} A_t = \sigma(1-\rho) E_t - \mu A_t \tag{55}$$

$${}_0^{CF}D_t^{\alpha} T_t = \nu_1 I_t - Q_3 T_t \tag{56}$$

To minimize the complexity, we remodel our equations as

$$ {}_{0}^{CF}D_t^{\alpha} S_t = F_S(t, S_t, E_t, I_t, A_t, T_t) \tag{57} $$
$$ {}_{0}^{CF}D_t^{\alpha} E_t = F_E(t, S_t, E_t, I_t, A_t, T_t) \tag{58} $$
$$ {}_{0}^{CF}D_t^{\alpha} I_t = F_I(t, S_t, E_t, I_t, A_t, T_t) \tag{59} $$
$$ {}_{0}^{CF}D_t^{\alpha} A_t = F_A(t, S_t, E_t, I_t, A_t, T_t) \tag{60} $$
$$ {}_{0}^{CF}D_t^{\alpha} T_t = F_T(t, S_t, E_t, I_t, A_t, T_t) \tag{61} $$

where the functions are defined as:

$$ F_S(t, S_t, E_t, I_t, A_t, T_t) = \pi - [\beta(I_t + \phi_1 T_t + \phi_2 A_t) + \mu] S_t \tag{62} $$
$$ F_E(t, S_t, E_t, I_t, A_t, T_t) = \beta(I_t + \phi_1 T_t + \phi_2 A_t) S_t - Q_1 E_t \tag{63} $$
$$ F_I(t, S_t, E_t, I_t, A_t, T_t) = \sigma\rho E_t - Q_2 I_t \tag{64} $$
$$ F_A(t, S_t, E_t, I_t, A_t, T_t) = \sigma(1-\rho) E_t - \mu A_t \tag{65} $$
$$ F_T(t, S_t, E_t, I_t, A_t, T_t) = \nu_1 I_t - Q_3 T_t \tag{66} $$

The corrected scheme with consistent parameter indexing develops:

$$ \begin{aligned} S_t^{m+1} = S_t^m &+ \frac{1-\alpha}{M(\alpha)}[F_S(t_{m+1}, \mathbf{X}^{m+1}) - F_S(t_m, \mathbf{X}^m)] \\ &+ \frac{\alpha\Delta t}{12M(\alpha)}[23F_S(t_m, \mathbf{X}^m) - 16F_S(t_{m-1}, \mathbf{X}^{m-1}) + 5F_S(t_{m-2}, \mathbf{X}^{m-2})] \\ &+ (\Lambda_{11} S_t^m + \Lambda_{12}) S_t^m \sqrt{\Delta t}\xi_1^{m+1} \end{aligned} \tag{67} $$

$$ \begin{aligned} E_t^{m+1} = E_t^m &+ \frac{1-\alpha}{M(\alpha)}[F_E(t_{m+1}, \mathbf{X}^{m+1}) - F_E(t_m, \mathbf{X}^m)] \\ &+ \frac{\alpha\Delta t}{12M(\alpha)}[23F_E(t_m, \mathbf{X}^m) - 16F_E(t_{m-1}, \mathbf{X}^{m-1}) + 5F_E(t_{m-2}, \mathbf{X}^{m-2})] \\ &+ (\Lambda_{21} E_t^m + \Lambda_{22}) E_t^m \sqrt{\Delta t}\xi_2^{m+1} \end{aligned} \tag{68} $$

$$ \begin{aligned} I_t^{m+1} = I_t^m &+ \frac{1-\alpha}{M(\alpha)}[F_I(t_{m+1}, \mathbf{X}^{m+1}) - F_I(t_m, \mathbf{X}^m)] \\ &+ \frac{\alpha\Delta t}{12M(\alpha)}[23F_I(t_m, \mathbf{X}^m) - 16F_I(t_{m-1}, \mathbf{X}^{m-1}) + 5F_I(t_{m-2}, \mathbf{X}^{m-2})] \\ &+ (\Lambda_{31} I_t^m + \Lambda_{32}) I_t^m \sqrt{\Delta t}\xi_3^{m+1} \end{aligned} \tag{69} $$

$$ A_t^{m+1} = A_t^m + \frac{1-\alpha}{M(\alpha)}[F_A(t_{m+1}, \mathbf{X}^{m+1}) - F_A(t_m, \mathbf{X}^m)] $$

$$
\begin{aligned}
&+ \frac{\alpha\Delta t}{12M(\alpha)}[23F_A(t_m, \mathbf{X}^m) - 16F_A(t_{m-1}, \mathbf{X}^{m-1}) + 5F_A(t_{m-2}, \mathbf{X}^{m-2})] \\
&+ (\Lambda_{41}A_t^m + \Lambda_{42})A_t^m\sqrt{\Delta t}\xi_4^{m+1} \qquad (70)
\end{aligned}
$$

$$
\begin{aligned}
T_t^{m+1} = T_t^m &+ \frac{1-\alpha}{M(\alpha)}[F_T(t_{m+1}, \mathbf{X}^{m+1}) - F_T(t_m, \mathbf{X}^m)] \\
&+ \frac{\alpha\Delta t}{12M(\alpha)}[23F_T(t_m, \mathbf{X}^m) - 16F_T(t_{m-1}, \mathbf{X}^{m-1}) + 5F_T(t_{m-2}, \mathbf{X}^{m-2})] \\
&+ (\Lambda_{51}T_t^m + \Lambda_{52})T_t^m\sqrt{\Delta t}\xi_5^{m+1} \qquad (71)
\end{aligned}
$$

where $\mathbf{X}^m = (S_t^m, E_t^m, I_t^m, A_t^m, T_t^m)$ and $\xi_i^{m+1} \sim \mathcal{N}(0,1)$ are independent standard normal random variables.

5.6. Convergence and Stability Analysis

The modified scheme inherits the convergence properties of the Adams-Bashforth method. Under the local Lipschitz conditions established in Section 4.1, the scheme maintains numerical stability. The three-step Adams-Bashforth approximation provides third-order accuracy for the integral terms, while the overall scheme maintains consistency with the fractional derivative formulation.

The corrected parameter indexing ensures that each compartment evolves according to its designated noise parameters, eliminating the inconsistency that could lead to incorrect stochastic dynamics. The time-state matching correction prevents the accumulation of numerical errors that could destabilize long-term simulations.

6. Results and Discussion

To acknowledge the theoretical results explained in the previous sections, we use numerical computations. For this purpose, a MATLAB program was written to acquire the indispensable optimality constraints, and a meaningful output is extensively tested using a range of simulations. We now better understand a practical case study with various numerical assumptions and parameter settings to highlight the dynamic structure of our infectious disease model. Table 2 shows the specific parameter values that we used. We used the fractional-order α to adopt a new model's significant parameters and demonstrated simulation results to better understand the model's qualitative behavior and the influence of the parameter on the system and viable control. We visualized the proposed coronavirus model for six different α values.

The improved fractional-order $S_tE_tA_tI_tT_tR_t$ model is used for COVID-19, with $\alpha = 0.92, 0.94, 0.96, 0.98, 1$. When $\alpha = 1$ is considered, the description of first-order updated $S_tE_tA_tI_tT_tR_t$ is accomplished. The first-order stochastic revised $S_tE_tA_tI_tT_tR_t$ model is then implemented, followed by the fractional-order stochastic proposed $S_tE_tA_tI_tT_tR_t$ model having order $\alpha = 0.92, 0.94, 0.96, 0.98, 1$.

Table 2: Summary of the variables with description.

Symbol	Definition
π	Rate of recruitment
β	Rate of transmission
μ	Rate of individual mortality
ϕ_1, ϕ_2	Infectiousness mitigation parameters
σ	Rate from exposed to infectious
ρ	Proportion developing symptoms
α	Recovery rate from treatment
ν_1, ν_2	Progress rates from I to T and R

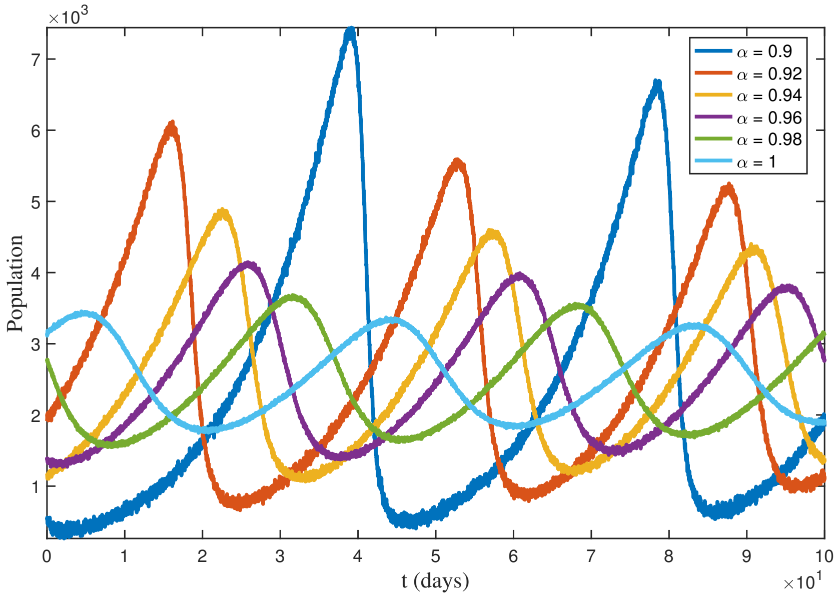

Figure 2: Dynamics time plots of the susceptible population for different values of α.

In Fig. 2, we plot the susceptible population for multiple values of α. It is explored that the susceptible population is decreased with the slightly increasing value of α. The exposed population graph is shown in Fig. 3. Fractional order α is an increasing function of the exposed population. Infectious symptomatic and asymptomatic population behaviors are observed in Figs. 4 and 5. It is noted that symptomatic and asymptomatic patients is rapidly decreasing when the parameter α is increasing slightly. The treated population class is shown in Fig. 6. It is depicted that the treated patients are increasing as the value of α decreases. From Fig. 7, it is also noted that the recovered population becomes more when the fractional order value of α is a decreasing function.

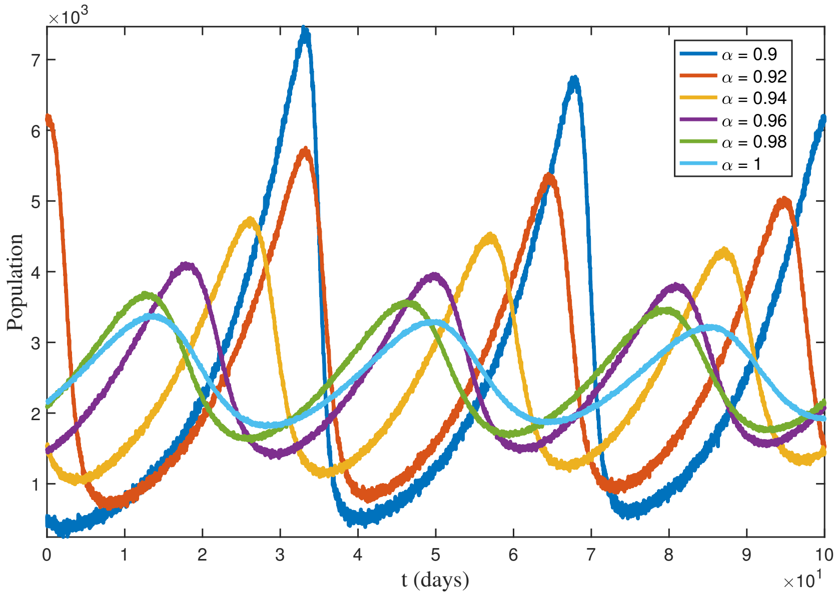

Figure 3: Dynamics time plots of the exposed population E_t for different values of α.

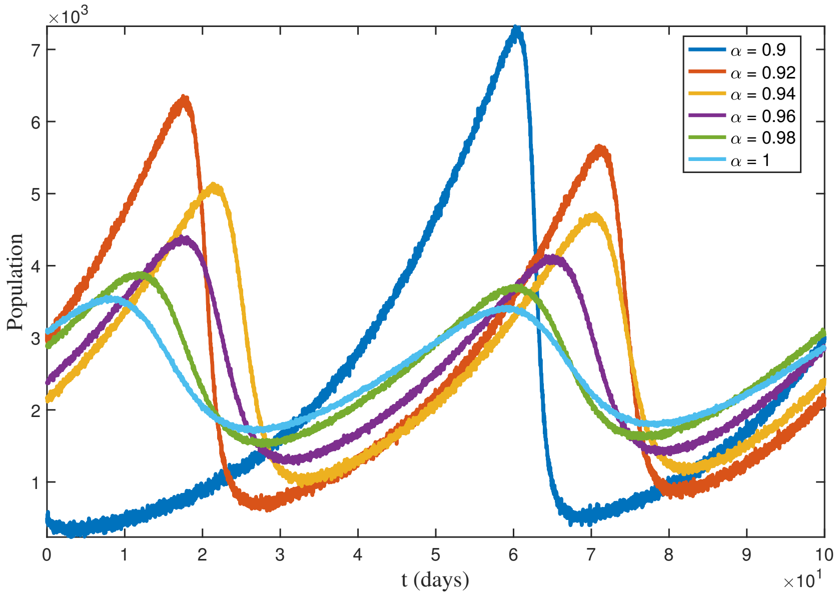

Figure 4: Dynamics time plots of the infectious symptomatic population I_t for different values of α.

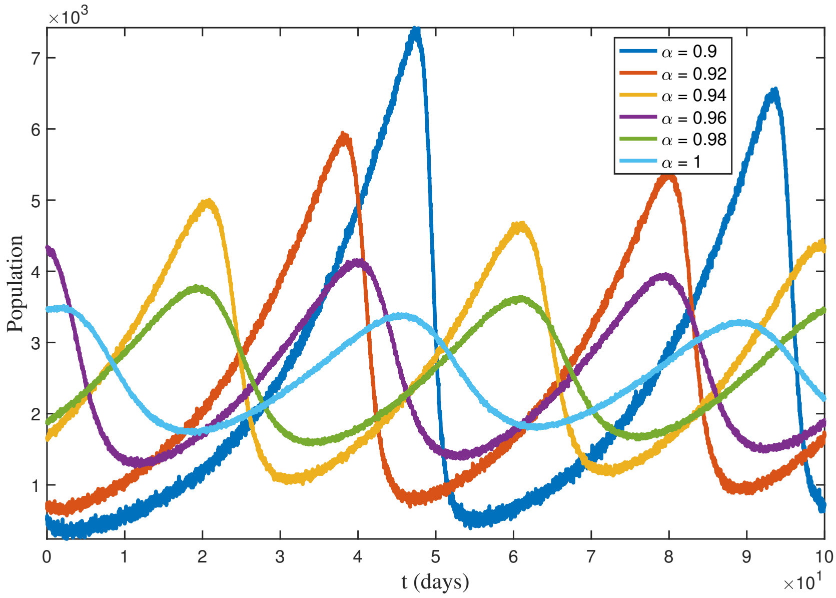

Figure 5: Dynamics time plots of the infectious asymptomatic population A_t for different values of α.

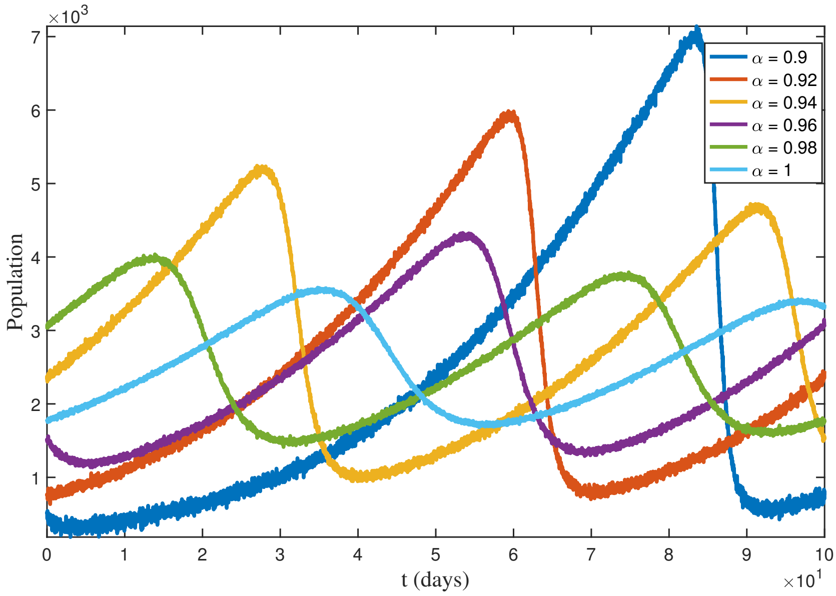

Figure 6: Dynamics time plots of the treated population T_t for different values of α.

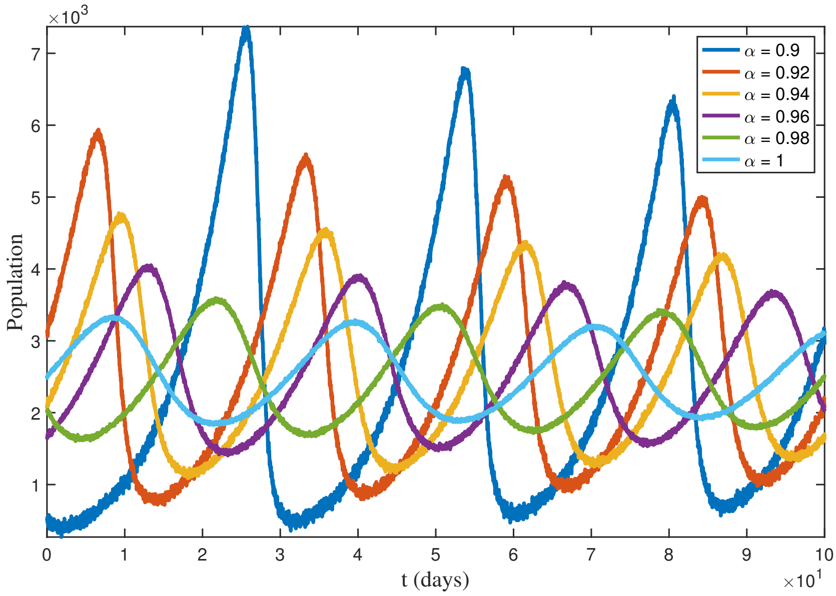

Figure 7: Dynamics time plots of the recovered population R_t for different values of α.

As a conclusion, decreases in the total number of hospitalized and chronically ill patients become increasingly significant as fractional-order α values decrease. As a result of the above graphical explanation, the likelihood of COVID-19 transmission can be lessened by constantly monitoring Standard Operating Procedures (SOPs) to dissuade confirmed contact between infectious and vulnerable people. The simulations are being shown for six distinct values of α, and the same phenomena were observed for different parameter values, acknowledging the fall in infected people is comparable quicker than normal for lower values of α.

For all fractional-order α values, the same conclusions have been drawn. The variance in the patients infected is found to be slightly feasible as α declines. When the fractional-order α is reduced, the susceptible population continues to rise, whereas the number of people in the other classes diminishes rapidly.

7. Conclusion

In this study, the fractional order derivatives that tend to be highly ubiquitous and provide a profound understanding of the potential issues are discussed. These fractional-order derivatives can encapsulate diminishing memory and crossover behavior, which are common in biomathematical systems such as viral infections. In the current work, we incorporated a hybrid fractional differential modeling with the help of the Caputo scheme, which is the most frequently applied operator in modeling, to understand the dynamics of COVID-19. The Caputo fractional approach for COVID-19 is first introduced, and later its essential nonlinear mathematical features, such as the system's stability and validity, as well as its solution, are comprehensively described. To elaborate on graphical interpretations, we investigated diverse scenarios of fractional order and stochastic noise. Since the assemblage of noise and the fractional-order model parameters are taken into account, the graphical results show the model's new graphical behavior. These novel observations will open up new avenues for research on the subject of stochastic equations, making them more valuable to scholars and researchers who are already acquainted with fractional stochastic differential equations.

From the results collected in this paper, we determine that the recommended hybrid stochastic model is more robust and better suitable for researching COVID-19 than the other Stochastic models. Simulations are provided that confirm our theoretical findings. Finally, we propose that academics and researchers might find our current discoveries to be a helpful tool.

Availability of Data and Material

No data was needed to perform this research.

Competing Interests

The authors declare that they have no competing interests.

Funding

No funding is available for this paper.

Authors' Contributions

All authors have read and approved this article. All authors have an equal contribution.

Acknowledgements

School of Mathematics and Statistics, Nanjing University of Information Science and Technology, 210044; and Reading Academy, Nanjing University of Information Science and Technology, Nanjing, P. R. China.

References

[1] K William and M Anderson. A contribution to the mathematical theory of epidemics. *Proc. R. Soc. A.*, 115:700–721, 1927.

[2] L Billard and P Dayananda. A multi-stage compartmental model for hiv-infected individuals: I–waiting time approach. *Math. Biosci.*, 249:92–101, 2014.

[3] A Atangana and S Araz. Extension of atangana-seda numerical method to partial differential equations with integer and non-integer order. *Alex. Eng. J.*, 59:2355–2370, 2020.

[4] A Atangana and S Araz. Modeling and forecasting the spread of covid-19 with stochastic and deterministic approaches: Africa and europe. *Adv. Differ. Equ.*, 57:1–107, 2021.

[5] A Atangana and S Araz. Nonlinear equations with global differential and integral operators: Existence, uniqueness with application to epidemiology. *Results Phys.*, 20:103593, 2021.

[6] D Anwarud, L Yongjin, and L Qi. Viral dynamics and control of hepatitis b virus (hbv) using an epidemic model. *Alexandria Eng. J.*, 59:667–679, 2020.

[7] N Afia, S Manmohan, and L David. Numerical study of sars epidemic model with the inclusion of diffusion in the system. *Appl. Math. Comput.*, 229:480–498, 2014.

[8] U Ranjit, K Nitu, and R Hari. Modeling the spread of bird flu and predicting outbreak diversity. *Nonlinear Anal. RWA.*, 9:1638–1648, 2008.

[9] D Anwarud and L Yongjin. The complex dynamics of hepatitis b infected individuals with optimal control. *J. Syst. Sci. Complexity*, 33:1–23, 2020.

[10] K William and M Anderson. Contributions to the mathematical theory of epidemics. ii.–the problem of endemicity. *Proc. R. Soc. A.*, 138:55–83, 1932.

[11] D Jaouad, A Karam, and H Zakia. Mathematical analysis of a fractional differential model of hbv infection with antibody immune response. *Chaos Soliton Fract.*, 136:109787, 2020.

[12] W Edmunds, G Medley, and D Nokes. The transmission dynamics and control of hepatitis b virus in the gambia. *Stat. Med.*, 18:2215–2233, 1996.

[13] D Anwarud, L Yongjin, K Tahir, and Z Gul. Mathematical analysis of spread and control of the novel coronavirus (covid-19) in china. *Chaos Soliton Fract.*, page 110286, 2013.

[14] M Goyal, H Baskonus, and A Prakash. An efficient technique for a time-fractional model of lassa hemorrhagic fever spreading in pregnant women. *Eur. Phys. J. Plus*, 134:1–10, 2019.

[15] D Kumar, J Singh, M Al-Qurashi, and D Baleanu. A new fractional sirs-si malaria disease model with application of vaccines, anti-malarial drugs, and spraying. *Adv. Diff. Eq.*, 278:1–10, 2019.

[16] M Chinazzi, J Davis, M Ajelli, and C Gioannini. The effect of travel restrictions on the spread of the 2019 novel coronavirus (2019-ncov) outbreak. *Science*, 368:395–400, 2020.

[17] B Tang. An updated estimation of the risk of transmission of the novel coronavirus (2019-ncov). *Infect. Dis. Model*, 116:248–255, 2020.

[18] M Carletti. Mean-square stability of a stochastic model for bacteriophage infection with time delays. *Math. Biosci.*, 210:395–414, 2007.

[19] M Jovanovic and M Krstic. Stochastically perturbed vector-borne disease models with direct transmission. *Appl. Math. Model*, 36:5214–5228, 2012.

[20] T Elisabetta, M Stefania, and V Pasquale. Stability of a stochastic sir system. *Phys.*

A., 354:111–126, 2005.

[21] R Hilfer. *Application of fractional calculus in physics*. World Scientific, 2011.

[22] E Ahmed and A Elgazzar. On fractional order differential equations model for nonlocal epidemics. *Phys. A.*, 379:607–614, 2007.

[23] A Carvalho and C Pinto. Non-integer order analysis of the impact of diabetes and resistant strains in a model for tb infection. *Commun. Nonlinear Sci. Numer.*, 61:104–126, 2018.

[24] C Pinto and A Carvalho. Diabetes mellitus and tb co-existence: Clinical implications from a fractional order modelling. *Appl. Math. Model.*, 68:219–243, 2019.

[25] J Singh, D Kumar, and D Baleanu. On the analysis of fractional diabetes model with exponential law. *Adv. Differ. Equ.*, 1:1–15, 2018.

[26] H Srivastava, V Dubey, R Kumar, J Singh, D Kumar, and D Baleanu. An efficient computational approach for a fractional-order biological population model with carrying capacity. *Chaos Soliton Fract.*, 138:109880, 2020.

[27] A Atangana and D Baleanu. New fractional derivatives with nonlocal and non-singular kernel: theory and application to heat transfer model. arXiv preprint 1602.03408, 2016.

[28] I Podlubny. *Fractional differential equations: an introduction to fractional derivatives, fractional differential equations, to methods of their solution and some of their applications*. Elsevier, 1998.

[29] D Baleanu, A Jajarmi, E Bonyah, and M Hajipour. New aspects of poor nutrition in the life cycle within the fractional calculus. *Adv. Differ. Equ.*, 1:1–14, 2018.

[30] M Altaf, M Azizah, and S Ullah. A fractional model for the dynamics of competition between commercial and rural banks in indonesia. *Chaos Soliton Fract.*, 122:32–46, 2019.

[31] S Ullah, M Altaf, M Farooq, Z Hammouch, and D Baleanu. A fractional model for the dynamics of tuberculosis infection using caputo-fabrizio derivative. *Discrete Contin. Dyn. Syst. S.*, page 975, 2019.

[32] M Altaf and A Atangana. Modeling the dynamics of novel coronavirus (2019-ncov) with fractional derivative. *Alex. Eng. J.*, 59:2379–2389, 2020.

[33] K Saad, J Aguilar, and A Almadiy. A fractional numerical study on a chronic hepatitis c virus infection model with immune response. *Chaos Soliton Fract.*, 139:110062, 2020.

[34] M Rahman, M Arfan, K Shah, and J Aguilar. Investigating a nonlinear dynamical model of covid-19 disease under fuzzy caputo, random and abc fractional order derivative. *Chaos Soliton Fract.*, 140:110232, 2020.

[35] M Altaf and F Aguilar. Tuberculosis model with relapse via fractional conformable derivative with power law. *Math. Methods Appl. Sci.*, 18:7113–7125, 2019.

[36] A Atangana and J Aguilar. Decolonisation of fractional calculus rules: breaking commutativity and associativity to capture more natural phenomena. *Eur. Phys. J. Plus*, 133:166, 2018.

[37] A Khan, J Aguilar, T Khan, and H Khan. Stability analysis and numerical solutions of fractional order hiv/aids model. *Chaos Soliton Fract.*, 122:119–128, 2019.

[38] V Morales, J Aguilar, K Saad, M Khan, and P Agarwal. Analytic solution for oxygen

diffusion from capillary to tissues involving external force effects: a fractional calculus approach. *Phys. A: Stat. Mech. Appl.*, 523:48–65, 2019.

[39] A Atangana. Modelling the spread of covid-19 with new fractal-fractional operators: Can the lockdown save mankind before vaccination? *Chaos Soliton Fract.*, 136:109860, 2020.

[40] D Baleanu, H Mohammadi, and S Rezapour. A fractional differential equation model for the covid-19 transmission by using the caputo–fabrizio derivative. *Adv. Differ. Equ.*, 1:1–27, 2020.

[41] N Tuan, H Mohammadi, and S Rezapour. A mathematical model for covid-19 transmission by using the caputo fractional derivative. *Chaos Soliton Fract.*, page 110107, 2020.

[42] F Salem. A mathematical model to investigate the transmission of covid-19 in the kingdom of saudi arabia. *Comput. Math. Methods. Med.*, 140:1–13, 2020.

[43] A Farooqi, R Ahmad, R Farooqi, A Nofal, and I Khan. A comparative epidemiological stability analysis of predictor-corrector type non-standard finite difference scheme for the transmissibility of measles. *Results Phys.*, 21:103756, 2021.

[44] R Ahmad, A Farooqi, and I Khan. An analytical approach to study the blood flow over a nonlinear tapering stenosed artery in flow of carreau fluid model. *Complex.*, 21:1–11, 2021.

[45] G Bary, W Ahmed, and I Khan. Regio- and stereoselective functionalization of alkenes with emphasis on mechanistic insight and sustainability concerns. *J. Saudi Chem. Soc.*, 25:101260, 2021.

[46] A Chauhan, S Kumar, and Y Karaca. A new fractional-order derivative-based nonlinear anisotropic diffusion model for biomedical imaging. *Chaos Theory Appl.*, 5:198–206, 2023.

[47] M El-Shorbagy, M Rahman, and Y Karaca. A computational analysis fractional complex-order values by abc operator and mittag-leffler kernel modeling. *Fractals*, 31:2340164, 2023.

[48] A Zarei, S Moradi, L Hosseinzadeh, MB Salavati, F Jalilian, M Shahlaei, K Sadrjavadi, and H Adibi. Synthesis, characterization, cytotoxic investigation of curcumin-based chromene derivatives and study of dna interaction via experimental and computational methods. *J. Mol. Struct.*, 1322:140331, 2025.